



Glucose production from hydrolysis of cellulose over a novel silica catalyst under hydrothermal conditions

Huayu Wang, Changbin Zhang*, Hong He*, Lian Wang

State Key Laboratory of Environmental Chemistry and Ecotoxicology, Research Center for Eco-Environmental Sciences, Chinese Academy of Sciences, Beijing 100085, China

Received 19 December 2010; revised 04 May 2011; accepted 20 May 2011

Abstract

A novel silica catalyst was synthesized by evaporation-induced self-assembly (EISA) method and tested for the catalytic selective hydrolysis of cellulose to glucose. This silica catalyst exhibited a higher catalytic activity than other oxides prepared by the same method, such as ZrO_2 , TiO_2 , and Al_2O_3 . Using silica as a catalyst, cellulose was selectively hydrolyzed into glucose with a glucose yield as high as 50% under hydrothermal conditions without hydrogen gas. The silica catalyst was characterized by Brunauer-Emmett-Teller (BET), X-ray diffraction (XRD) and transmission electron microscopy (TEM). The results of temperature-programmed desorption of ammonia (NH_3 -TPD) and textural properties indicated that the synergistic effect between strong acidity and a suitable pore diameter of the silica catalyst may be responsible for its high activity. In addition, the catalyst was recyclable and showed excellent stability during the recycle catalytic runs.

Key words: cellulose; glucose; silica catalyst; hydrolysis; hydrothermal; biomass

DOI: 10.1016/S1001-0742(11)60795-X

Introduction

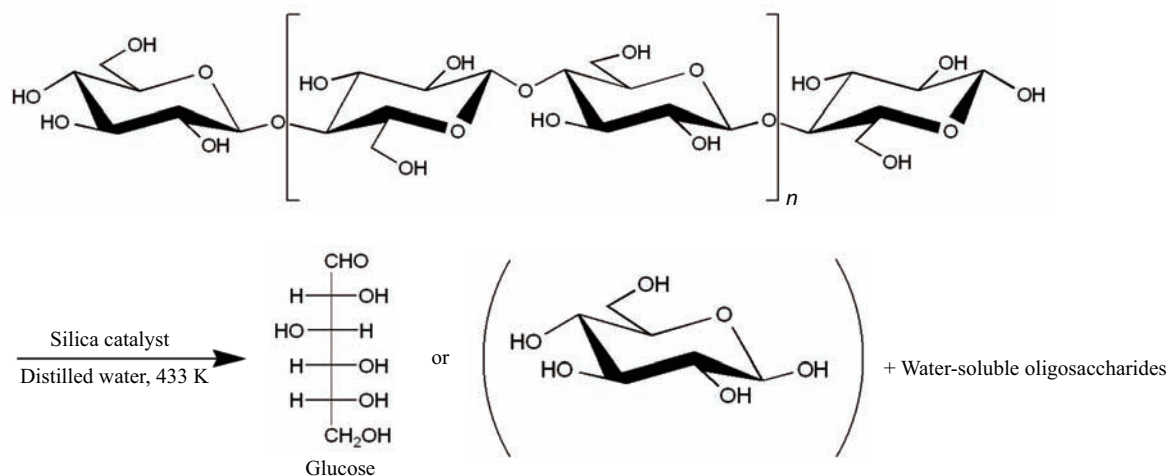
Diminishing petroleum reserves and growing concern about global climate change have stimulated the development of fuel production pathways based on renewable resources, such as starch, cellulose, and lignin. Among them, cellulose is by far the most abundant renewable biomass, with an annual production of approximately 1.5×10^{12} tons. Although the yield of starch is also very high, it is primarily used as a source of food (Klemm et al., 2005; Farrell et al., 2006; Deguchi et al., 2008). Establishing the efficient use of cellulose is generally recognized as a key technology.

Cellulose is a polysaccharide made of D-glucose connected together via β -1,4-glycosidic bonds. This connectivity results in various unique characteristics such as insolubility in common solvents (e.g. water) and structural rigidity. Furthermore, extensive hydrogen bonding networks formed between the cellulose chains in the crystals also arise from this linkage mode (Langan et al., 2001; Nishiyama et al., 2002, 2003). Consequently, the crystalline structure of cellulose is so robust that direct conversion of cellulose is always a challenging task.

Much research has focused on the degradation of cellulose with dilute acids (Mok et al., 1992), enzymes (Zhang and Lynd, 2004), and supercritical water (Saka and Ueno,

1999; Sasaki et al., 2000). Some major drawbacks of these methods include corrosion hazards, difficulties in separation, control of enzymes, danger to operators, and harsh reaction conditions. Recently, many researchers have sought to exploit cellulose using new technologies. For example, Fukuoka et al. (2006) reported that Pt/Al_2O_3 was an efficient catalyst for the conversion of cellulose into sugar alcohols in a water medium under hydrogen gas, while Luo et al. (2007) developed a two-step conversion of cellulose into polyols. A more recent example of catalytic conversion of cellulose was reported by Ji et al. (2008), who used $Ni-W_2C/AC$ as an effective catalyst to convert cellulose into ethylene glycol in a hydrogen atmosphere. Deng et al. (2009) demonstrated that Ru/CNT was an efficient catalyst for the direct conversion of cellulose to sorbitol in aqueous media. On the basis of the above studies, some catalytic processes for cellulose hydrolysis are known; however it is also evident that they have disadvantages, such as the need for hydrogen gas and/or the use of noble-metal catalysts. In an attempt to address these problems, recent research has examined the conversion of cellulose into glucose or saccharides using other solid acid catalysts, including a sulfonated activated-carbon catalyst (Onda et al., 2008) and amorphous carbon with a high density of sulfonic acid groups ($-SO_3H$) (Suganuma et al., 2008). Recently, heteropolyacids and polyvalent transition metal salts of $PW_{12}O_{40}^{3-}$ were found to act as effective heterogeneous catalysts for the selective hydrolysis of

* Corresponding author. E-mail: cbzhang@rcees.ac.cn (Changbin Zhang); honghe@rcees.ac.cn (Hong He)



Scheme 1 Catalytic conversion of cellulose into glucose and water-soluble oligosaccharides.

cellulose to saccharides (Shimizu et al., 2009). These pioneering works show that the acid sites for the hydrolysis of cellulose should mostly be *in situ*-generated H^+ -species, formed in the reaction medium or released from the solid material (Rinaldi and Schüth, 2009).

Here, we present the first observation that a novel silica catalyst exhibits high catalytic performance for the hydrolysis of cellulose into glucose under hydrothermal conditions with no hydrogen gas (Scheme 1). To our knowledge, no previous study has attempted to use this novel SiO_2 catalyst for high selective conversion of cellulose to glucose under hydrothermal conditions.

1 Materials and methods

1.1 Chemicals

Pluronic P123 ($M_{av} = 5800$, $\text{EO}_{20}\text{PO}_{70}\text{EO}_{20}$) was purchased from Sigma-Aldrich. Ethanol, tetraethyl orthosilicate (TEOS), zirconyl chloride octahydrate ($\text{ZrOCl}_2 \cdot 8\text{H}_2\text{O}$), tetrabutyl titanate ($\text{Ti}(\text{O}i\text{Bu})_4$) aluminum, iso-propoxide ($\text{Al}(\text{OPr})_3$), and nitric acid were purchased from Beijing Chemical Reagents. HZSM-5 ($\text{SiO}_2/\text{Al}_2\text{O}_3 = 25$) and HZSM-5 ($\text{SiO}_2/\text{Al}_2\text{O}_3 = 38$) were purchased from Nankai University, China. All other chemicals were used as received.

1.2 Catalyst preparation

The SiO_2 catalyst was prepared according to the evaporation-induced self-assembly (EISA) process (Yuan et al., 2008). Specifically, 0.5 g of Pluronic P123 was dissolved in 5 mL of ethanol and stirred for 4 hr. Then, 6 mmol of tetraethyl orthosilicate (TEOS) was added to the mixture, including 0.3 mL of nitric acid and 5 mL of ethanol. Once dissolved, the two solutions were combined and 2.5 mL of ethanol was used to thoroughly transfer the TEOS solution. The combined solution was stirred for a further 5 hr and transferred to an open Petri dish (diameter 8 cm). Solvent evaporation was performed at 313 K for 48 hr in air without stirring. After 48 hr aging, the gel product was dried at 373 K for 12 hr. Calcination was carried out by slowly increasing the temperature from room temperature

to 673 K (0.5 K/min ramping rate), and then heating at 673 K for 4 hr in air to remove the surfactant species.

For comparison, other catalysts containing ZrO_2 , TiO_2 , and Al_2O_3 were also prepared under the same conditions.

1.3 Characterization method

X-ray diffraction (XRD) was done using a computerized Rigaku D/max-RB Diffractometer ($\text{Cu } K\alpha$ radiation, 0.154056 nm; Rigaku, Japan) to obtain the XRD pattern. Scans were taken over a range of 2θ angles from 10° to 90° at a speed of $4^\circ/\text{min}$.

Brunauer-Emmett-Teller (BET) analysis was carried out on nitrogen adsorption-desorption isotherms at 77 K over the whole range of relative pressures using a Quantasorb-18 automatic instrument (Quanta Chrome Instrument Co., Boynton Beach, USA). Specific areas were computed from these isotherms using the BET method.

Transmission electron microscopy (TEM) characterizations were carried out using an H-7500 (Hitachi, Japan) instrument coupled with an energy dispersive X-ray (EDX) attachment. The accelerating voltage for the microscope was 80 kV and the point resolution was 0.36 nm.

High resolution transmission electron microscopy (HRTEM) was recorded digitally with a Gatan slow-scan charge-coupled device (CCD) camera on a JEOL-2011 electron microscope operating at 200 kV.

Temperature-programmed desorption of ammonia (NH_3 -TPD) experiments were carried out in a flow of Ar ($30 \text{ cm}^3/\text{min}$) over 500 mg of the catalyst. Prior to the TPD experiment, all catalysts were pretreated at 673 K for 1 hr in a flow of 20% O_2/Ar to yield a clean surface, followed by cooling to room temperature. The samples were treated with 2530 ppm NH_3 ($30 \text{ cm}^3/\text{min}$) at ambient temperature for 1 hr and then purged with Ar for 30 min to flush out excess NH_3 . During each TPD experiment, the sample was heated at a rate of 10 K/min to the final temperature of 1073 K, and the m/z value of 15 was monitored online using a mass spectrometer (HPR20; Hiden Analytical, Warrington, UK).

The number of acid sites was calculated by acid-base titration. First, NaOH aqueous solution (0.01 mol/L, 20 mL) was added to a catalyst (0.04 g). The mixture was

then stirred for 2 hr at room temperature. After centrifugal separation, several drops of phenolphthalein solution were added to the filtrate and this solution was then titrated with HCl (0.01 mol/L) aqueous solution to neutrality.

1.4 Hydrolysis reaction

In a typical reaction procedure, cellulose (Avicel[®], microcrystalline, 50 mg; Merck, Germany) was treated by ball-milling for 4 days. The catalyst (150 mg) and water (10 mL) were put into a stainless autoclave lined with Teflon (100 mL) under air without stirring. The autoclave was heated at 433 K for 12 hr without stirring (5 K/min ramping rate). After the reaction, the liquid reaction mixture was centrifuged and the filtered solution was subjected to high-performance liquid chromatography analysis (HPLC, RI detector, Waters 2414) equipped with a Sugar-Pak-1 column (6.5×300 mm) using water as a mobile phase. Cellulose conversions were determined by the change in cellulose weight before and after the reaction, with an uncertainty of ±3%. The hydrolysis product yield of glucose (R_g) and oligosaccharides (R_o) was calculated from Eqs. (1) and (2):

$$R_g = n_g/n_t \times 100\% \quad (1)$$

$$R_o = n_o/n_t \times 100\% \quad (2)$$

where, n_g (mol) is amount of glucose produced by the hydrolysis, n_t (mol) is total amount of glucose monomer in cellulose, and n_o (mol) is the amount of glucose monomer in oligosaccharides.

2 Results and discussion

2.1 Catalytic conversion of cellulose over metal oxide and solid acid catalysts

The results of cellulose conversion and selectivity of the major products over different catalysts are summarized in Table 1. This novel silica catalyst showed a remarkably high yield of glucose from cellulose under hydrothermal conditions, with 73.3% cellulose conversion and 50.1% glucose yield achieved at 433 K with a reaction time of 12 hr (Table 1, entry 8). Generally, the final major product of glucose is a useful carbohydrate (Takagaki et al., 2008; Dhepe et al., 2005; Suganuma et al., 2008). In addition to the main product of glucose, other products such as various

oligosaccharides and trace amounts of unknown products were also detected by HPLC. The carbon balance, based on total organic carbon (TOC) analysis of the liquid products, showed that almost no gas-phase product was produced (data not shown).

For comparison, ordered mesoporous SBA-15 material of hexagonal-ordered pore structure, prepared according to the literature (Zhao et al., 1998), and commercially available HZSM-5(25) and HZSM-5(38) catalysts were also tested, together with ZrO₂, TiO₂, and Al₂O₃. All catalysts were evaluated under the same conditions. When the self-made ZrO₂, TiO₂, and Al₂O₃, rather than SiO₂, were used in the catalytic experiment, the selectivity of glucose dramatically decreased (Table 1, entries 2–4). It has been reported that H-form zeolites can be used as solid catalysts for the hydrolysis of soluble oligosaccharides (Abadi et al., 1998), but this kind of H-form zeolite, such as HZSM-5(25) and HZSM-5(38), were poorly active (about 12% conversion) in the hydrolytic reaction of cellulose in our experiments (Table 1, entries 6 and 7). Another catalyst, SBA-15, also did not achieve appreciable activity in this reaction (Table 1, entry 5).

2.2 NH₃-TPD

Temperature-programmed desorption of ammonia (NH₃-TPD) was used to characterize the acidic properties of the tested samples. The NH₃-TPD profiles of samples are shown in Fig. 1. The desorption temperature indicates the acid strength of the sample: i.e., the higher the desorption temperature, the stronger the acid strength. The number of acid sites was estimated by conventional acid-base titration (Table 2). The ZrO₂ catalyst showed one broad peak of NH₃ desorption at about 398 K. The TiO₂ sample gave a twin peaks profile, indicating the presence of two types of NH₃-adsorbing sites of weak and medium strength. In comparison with TiO₂, the NH₃-TPD profile of the Al₂O₃ catalyst was composed of two distinct peaks. One peak appeared at around 383 K, followed by a broad and long-tailed signal at medium high temperature, ascribed to the presence of weak and moderate acid sites, and another appeared from 850 to 950 K. These are typically known as Lewis acid sites. Although Al₂O₃ has Lewis acidity, Brønsted acid sites are usually responsible for the acid-catalyzed hydrolysis reaction of cellulose. For SBA-15, we found one distinct NH₃ desorption peak sample at around

Table 1 Cellulose conversion and yield of products over different catalysts at 433 K for 12 hr^a

| Entry | Catalyst | Conversion (%) | Yield (%) | | | | | | |
|-------|---|----------------|-------------|---------------|---------------|-------------|------------|---------|------------------|
| | | | Cellohexose | Cellopentaose | Cellotetraose | Cellotriose | Cellobiose | Glucose | Unknown products |
| 1 | Blank | 4.5 | 1.3 | – | – | 0.3 | 0.2 | – | 2.7 |
| 2 | ZrO ₂ ^b | 15.8 | – | – | – | 0.1 | 0.3 | 9.0 | 6.4 |
| 3 | TiO ₂ ^b | 15.4 | 1.9 | – | 0.8 | 1.0 | 2.0 | 2.2 | 7.5 |
| 4 | Al ₂ O ₃ ^b | 17.0 | 5.3 | – | 1.2 | 0.1 | 1.3 | 0.1 | 9.0 |
| 5 | SBA-15 | 4.0 | 1.2 | – | 0.2 | 0.3 | 0.5 | 1.4 | 0.4 |
| 6 | HZSM-5(25) | 12.8 | – | 1.9 | 1.5 | 1.1 | 0.8 | 1.6 | 5.9 |
| 7 | HZSM-5(38) | 12.3 | – | 1.9 | 1.4 | 1.1 | 0.8 | 1.8 | 5.3 |
| 8 | SiO ₂ | 73.3 | 1.8 | – | 1.0 | 1.8 | 4.0 | 50.1 | 14.6 |

^a Reaction conditions: 12 hr reaction time; 10 mL H₂O; 0.05 g cellulose; 0.15 g catalyst.

^b Unless otherwise noted, the reactions of catalysts were carried out under identical experimental conditions to that of entry 8.

“–”: nondetectable amounts.

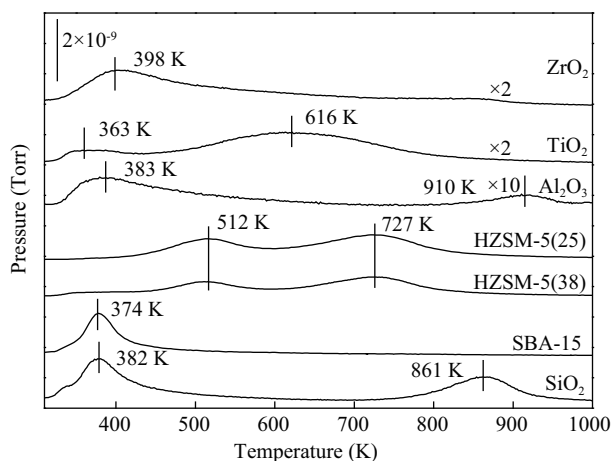


Fig. 1 Temperature-programmed desorption of ammonia (NH_3 -TPD) profiles for various samples.

Table 2 Textural properties of solid acid catalysts

| Catalyst | Surface area (m^2/g) | Average pore diameter (nm) | Pore volume (cm^3/g) | Acid amount (mmol/g) |
|--------------------------------|--|----------------------------|--|----------------------|
| ZrO ₂ | 135.5 | 2.770 | 0.089 | 0.08 |
| TiO ₂ | 272.9 | 2.535 | 0.264 | 0.09 |
| Al ₂ O ₃ | 344.8 | 5.836 | 0.628 | 0.10 |
| HZSM-5(25) | 317.1 | 0.443 | 0.624 | 0.38 |
| HZSM-5(38) | 331.2 | 0.449 | 0.690 | 0.41 |
| SBA-15 | 743.1 | 4.424 | 0.777 | 0.13 |
| SiO ₂ | 671.4 | 3.512 | 0.345 | 1.96 |

374 K, a weak acid site. As shown in Fig. 1, HZSM-5(25) exhibited two distinct broad peaks at around 512 K and 727 K. The first peak arose due to the weak acid sites present as surface hydroxyl groups. The strong peak at 727 K may have been related to the framework acidity (Wang et al., 2006). A similar curve was also observed for HZSM-5(38). Evidently, the desorption temperature of HZSM-5 was much higher than that of SBA-15. Likewise, the SiO₂ sample clearly showed the higher desorption temperature of strong acid sites, primarily signifying Brønsted acid sites. These results indicate that the acidic properties of the SiO₂ sample were stronger than those of the other samples. Generally, a higher activity in cellulose hydrolysis can be anticipated from a higher acid amount and a stronger acid strength. Nonetheless, the order of the peaks of these solid acid catalysts was not entirely consistent with that of the catalytic activity.

2.3 Textural properties

The textural properties of catalysts are also shown in Table 2. By considering both the results of NH_3 -TPD and textural properties of catalysts, we suggest that the cellulose molecule was hydrolyzed by the acid site around an appropriate pore window or on the surface of the catalyst, and the resulting smaller fragments entered into the pore to be converted. Although HZSM-5 has strong acidity in the framework structure, neither the glucose molecule ($0.50 \times 0.57 \times 0.58$ nm) (Rinaldi and Schüth, 2009) nor oligosaccharides can enter the channels and interact with the acid sites. The small average pore diameter of HZSM-5(25), about 0.443 nm, may be responsible

for the low activity. Moreover, the catalytic activity of HZSM-5(38) was similar to that of HZSM-5(25); they both had small average pore diameters. In contrast, SiO₂ had an appropriate average pore diameter (3.512 nm) that facilitated the transportation of oligosaccharides and thus enhanced the chances of oligosaccharides interacting with acid sites. Accordingly, oligosaccharides in the shape of a chain may enter the pore to be hydrolyzed. This is probably because strong acidity exists in its inner framework and moderate pore window. Conversely, SBA-15 had a large and ordered channel structure, but its acidity was very weak so that it did not boost the efficiency of the hydrolytic reaction of cellulose. A similar situation may occur with ZrO₂, TiO₂, and Al₂O₃. These results indicate that the high activity of the self-made SiO₂ catalyst may be due to a synergetic effect between strong acidity and a suitable pore diameter. A more detailed study is necessary to reveal the interaction mechanism of the catalyst and cellulose.

2.4 Characterization of self-made silica

We focused on the characterization of the self-made silica. Figure 2 shows the XRD pattern of the self-made silica catalyst, which showed no obvious sharp X-ray diffraction peaks besides a broad bump over the range of 2θ angles from 10° to 90°. Such a characteristic broad peak implies amorphous silica catalysts (Silva and Airolidi, 1997).

Figure 3 shows the TEM image and EDX result of the SiO₂ catalysts prepared by EISA. The particle size of the SiO₂ catalyst was small ranging from 21 to 70 nm in diameter (200–300 particles were counted to calculate the particle diameter distribution). Further, the EDX analysis revealed that no impurities existed in the silica catalyst.

2.5 Catalyst recycle experiments

The novel SiO₂ catalyst was also used in recycling experiments (Fig. 4). After the first reaction was run using the catalyst at 433 K for 12 hr, the suspension was centrifuged and the supernatant solution was collected. The mixture, including the solid catalyst and the cellulose residue, was then washed with water. Next, fresh cellulose and water were added to the catalyst obtained and a second run was conducted, as was a third, using the same procedure. As shown in Fig. 3, the product yields in the second and third

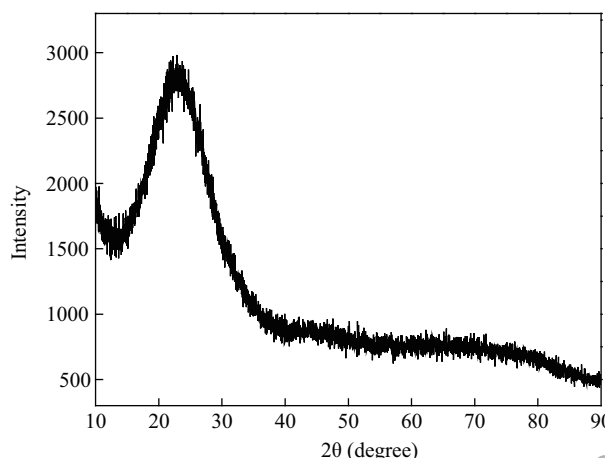


Fig. 2 XRD profile of the self-made silica.

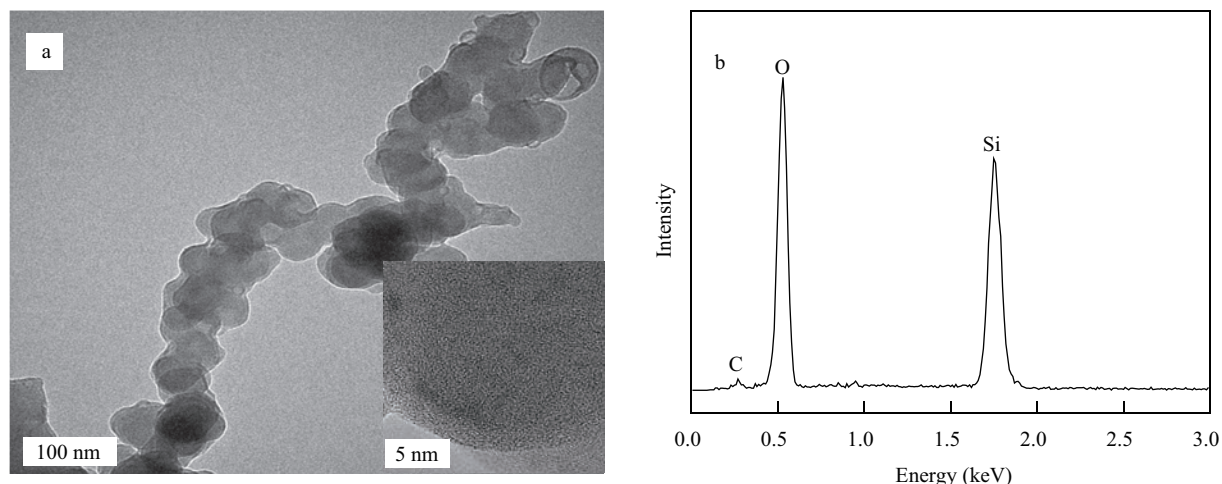


Fig. 3 (a) TEM images of the silica catalyst (the inserted image is HRTEM image) and (b) the energy dispersive X-ray spectroscopy (EDX) analysis results for (a).

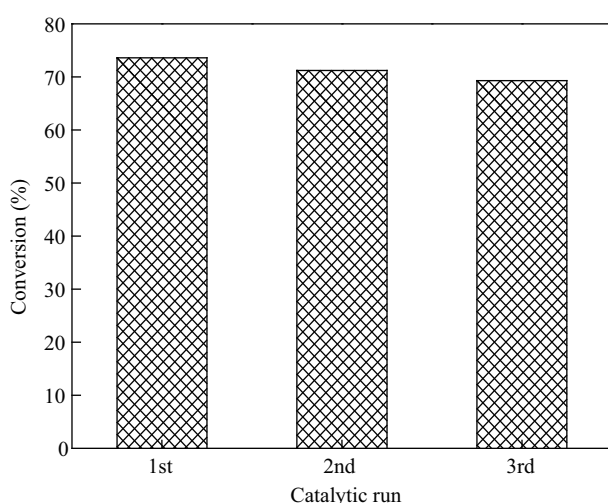


Fig. 4 Recycled catalytic runs. Reaction conditions: cellulose 0.05 g; catalyst 0.15 g; water 10 mL; autoclave reactor 100 mL; 433 K; 12 hr; air atmosphere.

runs were similar to that in the first run, with only slight losses. These results indicated that catalytic performance was not lost in the course of the catalytic runs.

Since catalyst stability evaluation is important for practical catalyst use, we further studied the stability of the SiO_2 catalysts in repeated runs. Considering the separating difficulty between the SiO_2 catalyst and cellulose residue, the SiO_2 catalyst was pretreated at 433 K for 12 hr, without adding cellulose. After the first pretreatment, the suspension was centrifuged and the SiO_2 catalyst was collected. A second pretreatment was then conducted using the same procedure. The pretreated SiO_2 catalysts were characterized by BET analysis. Table 3 depicts the results of the average pore diameter and pore volume of the fresh and pretreated SiO_2 catalysts. The surface area, average pore diameter, and pore volume of the catalysts changed little after pretreatment. The analysis data of the textural properties demonstrated that the SiO_2 catalyst had excellent stability during pretreatment.

Table 3 Textural stability properties of the pretreated SiO_2 catalysts

| Catalyst | Surface area (m^2/g) | Average Pore diameter (nm) | Pore volume (cm^3/g) |
|--------------------------------------|--|----------------------------|--|
| SiO_2^{a} | 671.4 | 3.512 | 0.345 |
| $\text{SiO}_2\text{-1st}^{\text{b}}$ | 669.3 | 3.501 | 0.342 |
| $\text{SiO}_2\text{-2nd}^{\text{c}}$ | 670.5 | 3.510 | 0.341 |

^a Fresh catalyst.

^b Catalyst after first pretreatment.

^c Catalyst after second pretreatment.

3 Conclusions

The results from this study demonstrated that the novel SiO_2 catalyst prepared by evaporation-induced self-assembly (EISA) method catalyzed the hydrolysis of cellulose with high selectivity into glucose in an environmentally friendly process. The catalyst was recyclable and the reproducible activity was achieved by a green process. More importantly, this catalyst is a non-precious metal catalyst and the reaction occurred in the absence of hydrogen gas. Thus, this work may open a new door for the use of cellulose in producing fuels and chemicals.

Acknowledgments

This work was supported by the National Natural Science Found for Creative Research Groups of China (No. 50921604).

References

- Abbadi A, Gotlieb K F, van Bekkum H, 1998. Study on solid acid catalyzed hydrolysis of maltose and related polysaccharides. *Starch*, 50(1): 23–28.
- Deguchi S, Tsujii K, Horikoshi K, 2008. Crystalline-to-amorphous transformation of cellulose in hot and compressed water and its implications for hydrothermal conversion. *Green Chemistry*, 10(2): 191–196.
- Deng W P, Tan X S, Fang W H, Zhang Q H, Wang Y, 2009. Conversion of cellulose into sorbitol over carbon nanotube-supported ruthenium catalyst. *Catalysis Letters*, 133(1-2): 167–174.

- Dhepe P L, Ohashi M, Inagaki S, Ichikawa M, Fukuoka A, 2005. Hydrolysis of sugars catalyzed by water-tolerant sulfonated mesoporous silicas. *Catalysis Letters*, 102(3–4): 163–169.
- Farrell A E, Plevin R J, Turner B T, Jones A D, O'Hare M, Kammen D M, 2006. Ethanol can contribute to energy and environmental goals. *Science*, 311(5760): 506–508.
- Fukuoka A, Dhepe P L, 2006. Catalytic conversion of cellulose into sugar alcohols. *Angewandte Chemie International Edition*, 45(31): 5161–5163.
- Ji N, Zhang T, Zheng M Y, Wang A Q, Wang H, Wang X D et al., 2008. Direct catalytic conversion of cellulose into ethylene glycol using nickel-promoted tungsten carbide catalysts. *Angewandte Chemie International Edition*, 47(44): 8510–8513.
- Klemm D, Heublein B, Fink H P, Bohn A, 2005. Cellulose: fascinating biopolymer and sustainable raw material. *Angewandte Chemie International Edition*, 44(22): 3358–3393.
- Langan P, Nishiyama Y, Chanzy H, 2001. X-ray structure of mercerized Cellulose II at 1 Å resolution. *Biomacromolecules*, 2(2): 410–416.
- Luo C, Wang S, Liu H C, 2007. Cellulose conversion into polyols catalyzed by reversibly formed acids and supported ruthenium clusters in hot water. *Angewandte Chemie International Edition*, 46(40): 7636–7639.
- Mok W S, Antal M J, Varhegyi G, 1992. Productive and parasitic pathways in dilute acid-catalyzed hydrolysis of cellulose. *Industrial and Engineering Chemistry Research*, 31(1): 94–100.
- Nishiyama Y, Langan P, Chanzy H, 2002. Crystal structure and hydrogen-bonding system in cellulose I β from synchrotron X-ray and neutron fiber diffraction. *Journal of the American Chemical Society*, 124(31): 9074–9082.
- Nishiyama Y, Sugiyama J, Chanzy H, Langan P, 2003. Crystal structure and hydrogen bonding system in cellulose I α from synchrotron X-ray and neutron fiber diffraction. *Journal of the American Chemical Society*, 125(47): 14300–14306.
- Onda A, Ochi T, Yanagisawa K, 2008. Selective hydrolysis of cellulose into glucose over solid acid catalysts. *Green Chemistry*, 10(10): 1033–1037.
- Rinaldi R, Schüth F, 2009. Design of solid catalysts for the conversion of biomass. *Energy & Environmental Science*, 2(6): 610–626.
- Saka S, Ueno T, 1999. Chemical conversion of various celluloses to glucose and its derivatives in supercritical water. *Cellulose*, 6(3): 177–191.
- Sasaki M, Fang Z, Fukushima Y, Adschiri T, Arai K, 2000. Dissolution and hydrolysis of cellulose in subcritical and supercritical water. *Industrial and Engineering Chemistry Research*, 39(8): 2883–2890.
- Shimizu K I, Furukawa H, Kobayashi N, Itaya Y, Satsuma A, 2009. Effects of Brønsted and Lewis acidities on activity and selectivity of heteropolyacid-based catalysts for hydrolysis of cellobiose and cellulose. *Green Chemistry*, 11(10): 1627–1632.
- Silva C R, Airoidi C, 1997. Acid and base catalysts in the hybrid silica sol-gel process. *Journal of Colloid and Interface Science*, 195(2): 381–387.
- Suganuma S, Nakajima K, Kitano M, Yamaguchi D, Kato H, Hayashi S et al., 2008. Hydrolysis of cellulose by amorphous carbon bearing SO₃H, COOH, and OH groups. *Journal of the American Chemical Society*, 130(38): 12787–12793.
- Takagaki A, Tagusagawa C, Domen K, 2008. Glucose production from saccharides using layered transition metal oxide and exfoliated nanosheets as a water-tolerant solid acid catalyst. *Chemical Communications*, (42): 5363–5365.
- Wang K Y, Wang X S, Li G, 2006. Quantitatively study acid strength distribution on nanoscale ZSM-5. *Microporous and Mesoporous Materials*, 94(1–3): 325–329.
- Yuan Q, Yin A X, Luo C, Sun L D, Zhang Y W, Duan W T et al., 2008. Facile synthesis for ordered mesoporous γ -aluminas with high thermal stability. *Journal of the American Chemical Society*, 130(11): 3465–3472.
- Zhang Y P, Lynd L R, 2004. Toward an Aggregated understanding of enzymatic hydrolysis of cellulose: noncomplexed cellulase Systems. *Biotechnology and Bioengineering*, 88(7): 797–824.
- Zhao D Y, Feng J L, Huo Q S, Fredrikson N, Fredrikson G H, Chmelka B F et al., 1998. Triblock copolymer syntheses of mesoporous silica with periodic 50 to 300 angstrom pores. *Science*, 279(5350): 548–552.